PERGAMON

Deep-Sea Research I 45 (1998) 1931–1954

DEEP-SEA RESEARCH
PART I

A method for estimating the flocculation time of monodispersed sediment suspensions

E.A. Gonzalez, P.S. Hill*

Department of Oceanography, Dalhousie University, Halifax, Novia Scotia, Canada B3H 4J1

Received 1 August 1997; accepted 11 February 1998

Abstract

A new method is presented for determining the flocculation time of monodispersed sediment suspensions. Flocculation time is the critical time at which abrupt changes in the particle size spectrum of an aggregative suspension occurs. This method predicts flocculation times to within 6% of values predicted by a geometric sectional aggregation model (Batterham, R.J., Hall, J.S. and Barton, G., 1981. In: Proceedings, 3rd International Symposium on Agglomeration, Nürnberg, Federal Republic of Germany, pp. A136–A150) but uses only a fraction of the computational effort. Flocculation times estimated in this way are superior to estimates of flocculation time scale made using half-life because particle geometry and differential settling encounter are taken into account. The proposed model is based on typical size distributions calculated using the Batterham *et al.* model. These size distributions have approximately equal mass in geometrically increasing size classes, i.e. they are Junge-dispersed. By assuming that the suspension remains Junge-dispersed throughout its evolution, the system of differential equations required to describe the suspension reduces to a single differential equation. Flocculation times are calculated for three values of maximum floc size ($d_{max} = \{10,1,0.1$ mm$\}$), a maximum settling velocity of $w_s = 1$ mm s^{-1}, and a variety of initial conditions. For a given set of inputs, flocculation times calculated in this way are linearly related to those calculated using the Batterham *et al.* model, but the slope of the relationship varies with fractal dimension. Multiple linear regression equations are developed to directly relate the two. The effect of including sinking losses into the Batterham *et al.* model is also investigated. If the sinking loss time scale is much longer than the flocculation time, then the suspension becomes flocculated at roughly the same time it would have had there been no sinking losses, and the new method can be used. Conversely, if the sinking time scale is less than or equal to the flocculation time, then the new method cannot be used.

*Corresponding author. Fax: 001 902 494 3877; e-mail: paul.hill@dal.ca.

0967-0637/98/$–see front matter
PII: S0967-0637(98)00045-4

1. Introduction

When the fate of particles in the water column is investigated, the importance of aggregation relative to other removal mechanisms, such as deposition, often is determined by comparison of time scales (McCave, 1985; Logan *et al.*, 1995). While deposition time scale is easily calculated, aggregation time scale is not. In any aggregating suspension, there is a wide range of particle sizes and types, and for each particle–particle interaction, there is a unique encounter rate. Numerical models that track the evolution of particle size distributions during aggregation (Lick *et al.*, 1992; Lick and Huang, 1993; Hill and Nowell, 1995) are rather difficult to implement and costly to run and, as such, are seldom used to calculate time scales. Instead, particle half-life, the time required for the initial particle number concentration to decrease by half, is used (Friedlander, 1977). Half-life models assume that when two particles coalesce the total volume of particles is conserved, and that the particle size distribution remains monodispersed, that is to say, all particles in suspension at any instant are the same size.

Lick *et al.* (1992) compare estimates of aggregation time scales calculated using half-life to aggregation times calculated using a numerical model and find that half-lives can be as much as 100 times larger than times predicted by the model. Bremer *et al.* (1995) also suggest that half-life is a poor estimate of aggregation time primarily because it ignores the effect of aggregate packing geometry. They address this effect by relaxing the assumption that total enclosed volume remains constant and deriving an algebraic expression for flocculation time. Their formulation maintains the assumption that the particle size distribution is monodispersed.

Because of the assumption of monodispersity, the Bremer *et al.* (1995) formulation is limited to aggregation caused by turbulent shear. However, for shear rates typically found in the ocean, particle encounter also occurs through differential settling of different-sized particles (McCave, 1984). Given the importance of aggregation in determining the fate of particulate matter in the sea (McCave, 1984, 1985; Jackson, 1990; Logan *et al.*, 1995), a clear need exists for a model of aggregation time that permits variable packing geometry and multiple particle sizes. To address this need, a new method is presented for calculating aggregation time based on a power-law distribution. Because a fixed form of the size distribution is assumed, this method is considerably faster and less complicated than the numerical models mentioned above.

2. Background

2.1. Typical suspension behaviour

In laboratory experiments, aggregating fine particle suspensions undergo abrupt transition from the unflocculated to the flocculated state (Oles, 1992; Lick and Huang, 1993; Spicer and Pratsinis, 1996). After a given time, during which median particle size remains close to its initial value, intense aggregation takes place, and median particle size increases exponentially until a steady state size is reached.

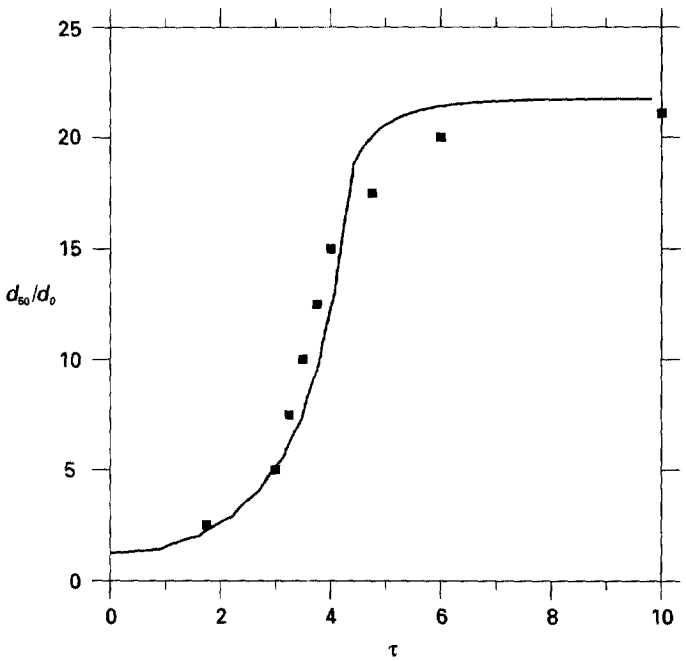

Fig. 1. Nondimensional median diameter (d_{50}/d_0) as a function of nondimensional time (τ) for an aggregating, fine sediment suspension showing experimental data from Oles (1992) (squares) overlayed with model output from Hill and Nowell (1995) (solid line).

Numerical, population-balance models of aggregation predict this behaviour (Lick *et al.*, 1992; Lick and Huang, 1993; and Hill and Nowell, 1995). Median diameter, d_{50}, of particles in suspension changes slowly until the flocculation time, after which d_{50} increases rapidly (Fig. 1). (In Fig. 1, the symbol τ is dimensionless time; it is defined in Eq. (11).) Because there is a clear transition between the two states, this behaviour lends itself to a step-function approximation of the form

$$d_{50} = \begin{cases} d_0 & \text{if } t < t_{\text{floc}}, \\ d_{\max} & \text{if } t \geqslant t_{\text{floc}}, \end{cases} \tag{1}$$

where d_0 is the initial mean diameter, $d_{\max}$ is the maximum floc diameter, and t_{floc} is the flocculation time. A simple method for estimating t_{floc} would allow for direct calculation of the most important information to come from aggregation models without the computational effort required to track the entire size distribution with time.

2.2. *Particle encounter mechanisms*

For particles larger than $d \sim 8\,\mu\text{m}$ and conditions representative of the ocean, differential settling and turbulent shear dominate particle encounter (McCave, 1984).

Differential settling encounter results when particles of different sizes or densities settle past one another under the force of gravity. Turbulent shear is the mechanism by which particles encounter one another through the action of turbulent eddies.

Particle encounter-rate coefficients can be broken into three parts so that (Hill *et al.*, 1992)

$$\beta_{ij} = \alpha_{ij} E_{ij} K_{ij}, \tag{2}$$

where α_{ij} is the sticking efficiency between particles of types i and j, E_{ij} is the contact efficiency between these particles, and K_{ij} is their encounter rate.

Encounter rates for differential settling and turbulent shear are (Pruppacher and Klett, 1980)

$$K_{i,j} = \frac{\pi}{4} (d_i + d_j)^2 |w_{s_j} - w_{s_i}|, \tag{3}$$

and (Saffman and Turner, 1956)

$$K_{i,j} = 0.16\, G (d_i + d_j)^3, \tag{4}$$

where w_{s_j} and w_{s_i} are the settling velocities of particles of types j and i, $G = (\varepsilon/\nu)^{1/2}$ is the shear rate[1], ε is the dissipation rate of turbulent kinetic energy, and ν is the kinematic viscosity of the suspending medium. These expressions show that encounter rates for both differential settling and turbulent shear encounter have a strong diameter dependence. Therefore, encounter rate coefficients between large particles are much greater than between small particles.

The stickiness of particles, quantified by their sticking efficiency, is the ratio of the rate at which particles stick to the rate at which they make contact. Particle stickiness is highly variable, ranging from $< 10^{-3}$ (Weilenmann *et al.*, 1989) to about 1 (Alldredge and McGillivary, 1991). Stickiness has been found to be sensitive to the presence of dissolved organic matter and the ionic strength of the suspending medium (Weilenmann *et al.*, 1989). It is assumed here to be independent of particle size.

Contact efficiency, E_{ij}, is the ratio of the rate at which particles make contact to the rate at which they encounter one another. The value of E_{ij} depends on the assumed model for particle encounter (Han and Lawler, 1992). In the "rectilinear" model, all hydrodynamic effects are ignored, and any two particles that encounter one another will make contact, or $E_{ij} = 1$. In the "curvilinear" model, particles are assumed to be solid spheres that follow streamlines, and E_{ij} is a function of the diameters of the interacting particles.

Recent experimental work by Li and Logan (1997a, b) demonstrates that neither model of particle contact accurately predicts observed contact efficiencies. For differential settling encounter, contact efficiencies are an order of magnitude higher than predicted by the curvilinear model and two orders of magnitude lower than predicted

[1]Although the symbol $\dot{\gamma}$ has been adopted for shear rate by the Society of Rheology (Dealy, 1984), the symbol G is used here in order to be consistent with oceanographic literature.

by the rectilinear model (Li and Logan, 1997a). For turbulent shear encounter, contact efficiencies are five orders of magnitude higher than predicted by the curvilinear model and two orders of magnitude lower than predicted by the rectilinear model (Li and Logan, 1997b). Li and Logan propose alternate expressions for $E_{i,j}$ as a function of particle size for differential settling and turbulent shear encounter. However, due to the complexity of these expressions and the need for unknown inputs, such as filtration efficiency, the simplifying assumption is made that $E_{i,j} = 0.01$ as suggested by their observations for both encounter mechanisms.

2.3. Settling velocity and fractal dimension

Large particles that result from the aggregation of smaller particles have random structures that can be characterized using fractal geometry (Meakin, 1991). Rather than coalescing to form particles with volumes equal to the sum of the volumes of their component particles, these "flocs" have enclosed volumes greater than the sum of their components. The relationship between the volume of solid material within a floc, v_s, and floc diameter, d, is given by (Logan and Wilkinson, 1990)

$$v_s = v_0\left(\frac{d}{d_0}\right)^{D3}, \tag{5}$$

where v_0 is the component grain volume, and $D3$ is the 3-D fractal dimension. If $D3 = 3$, then the particle is a coalesced sphere; if $D3 < 3$, then the particle is a floc and has an enclosed volume greater than that of its components.

The fractal dimension of marine flocs typically is determined by comparing floc settling velocities to diameters, e.g. Hill *et al.* (1997). Stokes Law gives the settling velocity of a sphere of density ρ_p and diameter d as

$$w_s = \frac{(\rho_p - \rho)gd^2}{18\mu}, \tag{6}$$

where g is the constant of gravitational acceleration, and ρ and μ are the density and dynamic viscosity of the surrounding medium (water). The excess density of a fractal aggregate $(\rho_p - \rho)$ is related to that of a coalesced sphere $(\rho_s - \rho)$ by

$$\rho_p - \rho = (\rho_s - \rho)\left(\frac{d}{d_0}\right)^{D3-3},$$

so that Eq. (6) becomes

$$w_s = \frac{(\rho_s - \rho)gd_0^2}{18\mu}\left(\frac{d}{d_0}\right)^{D3-1}. \tag{7}$$

It is assumed in this derivation that flocs behave as solid spheres and that Stokes Law still holds, and the drag coefficient, $C_d = 24/\mathrm{Re}$, where Re is the Reynolds Number, is unchanged. Dyer *et al.* (1996) report median settling velocities of 1 mm s^{-1} with a range of 0.1 to about 5 mm s^{-1}, and floc sizes in the range 50 to 1000 μm.

ten Brinke (1994), Syvitski *et al.* (1995) and Hill *et al.* (1997) also report floc diameters and settling velocities on the order of 1 mm and 1 mm s^{-1}, respectively. Based on Eq. (7), marine flocs have fractal dimensions in the range $1.5 \leqslant D3 \leqslant 2.5$ (ten Brinke, 1994; Hill *et al.*, 1997).

The fractal nature of flocs has a great effect on the aggregation process. Because flocs have larger encased volumes than coalesced particles, encounter rates are enhanced because of the strong diameter dependence of encounter-rate coefficients (see Eqs. (3) and (4)).

2.4. Estimates of flocculation time

The traditional definition of flocculation time is the half-life. If one assumes that a suspension remains monodispersed and that encased volume of particles in suspension remains constant ($D3 = 3$), then time rate of change of number concentration is first-order in concentration (Birkner and Morgan, 1968). First-order reactions can be characterized with a half-life, the expression for which is given by

$$t_{1/2} = \frac{\pi \ln 2}{0.16(24) G \phi_0}, \tag{8}$$

where ϕ_0 is the initial volume fraction of particles in suspension. By using half-life to calculate flocculation times, McCave (1984, 1985) and Logan *et al.* (1995) implicitly make these assumptions.

Bremer *et al.* (1995) draw attention to the fact that calculating flocculation times with half-life ignores the role of aggregate geometry. They present an alternate expression for flocculation time, which takes into account the fractal dimension of flocs but retains the assumption that the size distribution remains monodispersed. For $D3 < 3$, the flocculation time is given by

$$t_{\text{floc}} = \frac{\pi}{0.16(24)} \frac{D3}{3 - D3} G^{-1} \phi_0^{-1} (1 - q^{D3-3}), \tag{9}$$

where $q = d_c/d_0$, and d_c is some critical particle diameter. Bremer *et al.* (1995) define this critical size as the particle size above which the aggregation rate increases abruptly. At this time, macroscopic changes in the suspension occur, such as visible sedimentation. Flocculation times calculated using Eq. (9) are always shorter than half-lives because of the dependence on fractal dimension.

Because the size distribution is assumed to be monodispersed, Eq. (9) cannot be used to calculate the flocculation time of a suspension undergoing aggregation due to differential settling. All particles in a monodispersion settle at the same speed, so particles cannot overtake one another and make contact in that way. Simply ignoring this mechanism of particle encounter leads to inaccurate estimates of flocculation time, because differential settling is an important encounter mechanism in the sea. Therefore, a new method that assumes a different form for the size distribution is needed.

3. Methods

The aim of this work is to develop a method for estimating the time required for an aggregating suspension to go from the unflocculated to fully flocculated state, without the computational complexity of full numerical models. The criterion to be used is that the median diameter of particles in suspension is midway between the component grain diameter and the maximum diameter that flocs can attain. This criterion is an arbitrary one, but it allows for comparison among methods. In addition, the time interval over which the transition occurs is short compared to the flocculation time, so any reasonable criterion would give similar results.

3.1. Sectional model

In their review of zero-order coagulation models, Kostoglou and Karabelas (1994) report that models of the type proposed by Batterham *et al.* (1981) give the best overall performance. The model of Batterham *et al.* conserves particle mass, and it most closely approximates the analytical solutions for constant and sum encounter kernels. Also, its form is computationally efficient.

The Batterham *et al.* (1981) model is a discrete geometric sectional model. This means that the particle-size distribution is approximated by a histogram with a constant size distribution in each cell or section, and that section widths increase geometrically with particle volume. The size distribution is further simplified by assuming that only particles of discrete volumes may exist, so that particles in section j have volume equal to $2^{j-1}v_0$, where v_0 is the initial mean volume of particles in suspension.

According to the population balance approach, an ordinary differential equation expressing the rate of change of dimensionless particle number, n, with dimensionless time, τ, is required for each section. For section i, the Batterham *et al.* (1981) model states

$$\frac{\mathrm{d}n_i}{\mathrm{d}\tau} = \tfrac{3}{8}\hat{\beta}_{i-2,i-1}\,n_{i-2}n_{i-1} + \tfrac{3}{4}\hat{\beta}_{i-1,i}n_{i-1}n_i + \hat{\beta}_{i-1,i-1}n_{i-1}^2 + \sum_{m=1}^{i-2}\frac{2^i+2^m}{2^i}\hat{\beta}_{i,m}\,n_i n_m - \sum_{m=1}^{h-1} q_{i,m}\hat{\beta}_{i,m}\,n_i\,n_m,$$

$$q_{i,m} = \begin{cases} 2 & \text{if } i = m, \\ 1 & \text{otherwise,} \end{cases} \tag{10}$$

where for the sections below, only the indicated terms are used:

$i = 1$, fifth term,

$i = 2$, second, third and fifth terms,

$i = h$, first and third terms.

The coefficients $\hat{\beta}$ are dimensionless encounter-rate kernels, h is the number of sections, and

$$\tau = \beta(v_0, v_0) N_0 t, \tag{11}$$

where $\beta(v_0, v_0)$ is the encounter-rate kernel for particles in the first section, N_0 is the initial particle number concentration, and t is time. For a discussion of each term in Eq. (10), see Koh *et al.* (1987).

Dimensionless encounter-rate kernels, $\hat{\beta}$, are defined as

$$\hat{\beta}_{i,j} = \frac{\beta(v_i, v_j)}{\beta(v_0, v_0)}, \tag{12}$$

where $\beta(v_i, v_j)$ is the encounter-rate kernel for particles of volume v_i and v_j. The forms of $\beta(v_i, v_i)$ and $\beta(v_0, v_0)$ depend on encounter mechanism. To include the fractal nature of flocs, $\hat{\beta}$ is calculated using the diameter that a floc in section j must have if its solids volume is $2^{j-1}v_0$. Rearranging Eq. (5) for floc diameter gives

$$d = d_0 \left(\frac{v_s}{v_0}\right)^{1/D3},$$

or

$$d_j = d_0 \left(2^{j-1}\right)^{1/D3}. \tag{13}$$

Therefore, for a given value of j, the particle diameter in that class varies depending on the fractal dimension.

To simplify notation, the Batterham *et al.* model is referred to as the 'full' model, as opposed to the 'reduced' model to be proposed below, and the dimensionless flocculation time predicted by this model is represented by τ_B.

3.2. *Junge-dispersion estimate of flocculation time*

In situ observations of marine particles reveal that they are distributed such that there is equal mass in geometrically increasing size bins (Lerman *et al.*, 1977). This Junge distribution has the general form (Hunt, 1980)

$$f(d) = A d^{-b}, \tag{14}$$

where $f(d)$ is the number density function, and A and b are empirical constants. For a Junge distribution, $b = 4$. The number concentration, N, of particles from d to $d + \mathrm{d}d$ is given by (Hunt, 1980)

$$\mathrm{d}N = f(d)\,\mathrm{d}d.$$

Mass distributions predicted by the Batterham et al. model are also approximately Junge-distributed (see Fig. 2). Mass concentration is roughly equal for small sections,

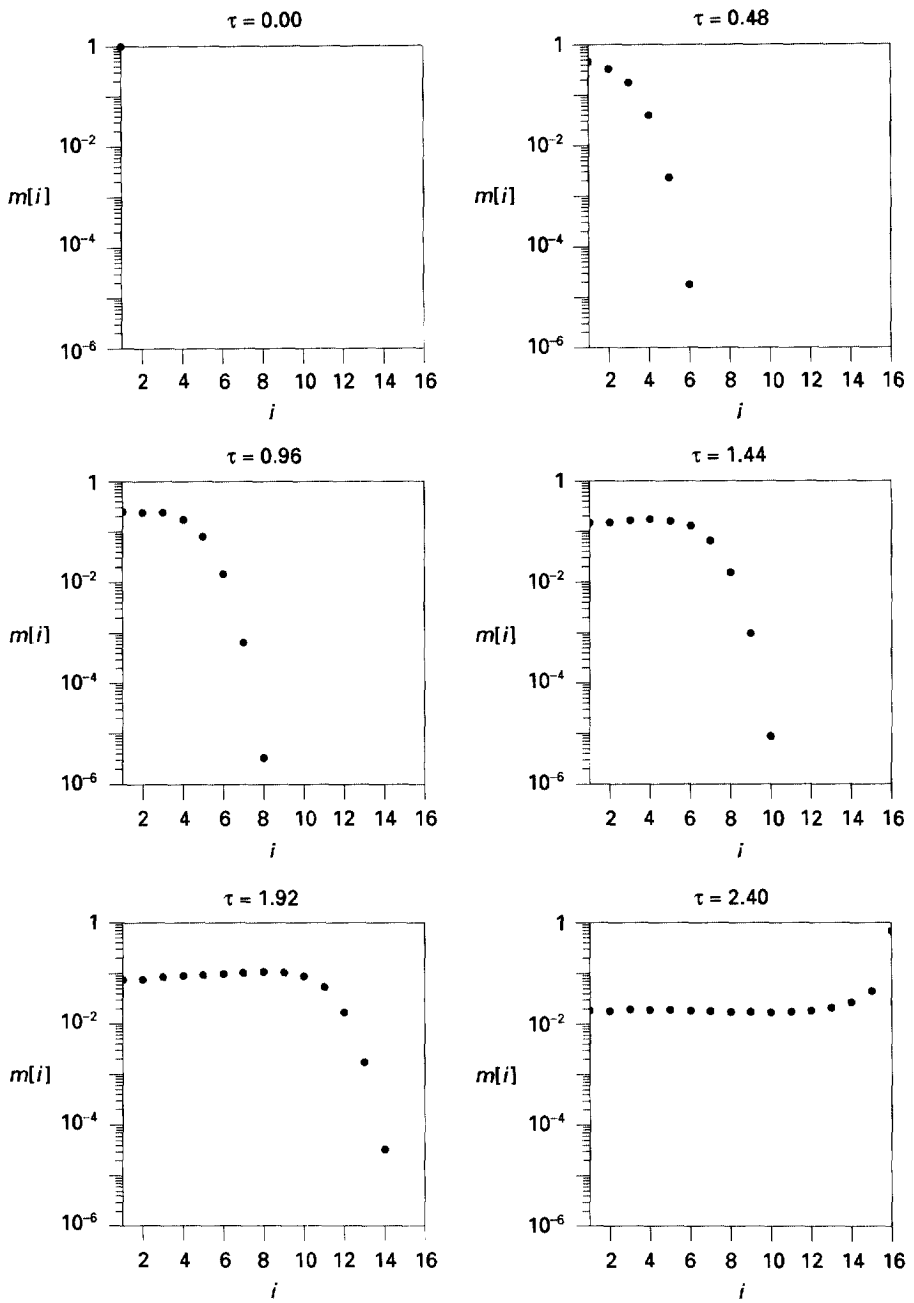

Fig. 2. Sample series of mass distributions. Each plot shows nondimensional mass concentration (m) in each section (i) at a given nondimensional time (τ). This case is for turbulent shear encounter with 16 sections and a fractal dimension $D3 = 2.0$ ($\tau_{floc} = 2.2$). The distribution shown in the last plot is an example of a Junge distribution, because it has approximately equal mass in each size class.

but drops off for larger sections. In addition, the series of particle size distributions shows that the system evolves as a Junge distribution. As aggregation proceeds, mass is lost equally from the small sections and transferred into larger sections so that the mass distribution remains flat.

A method of estimation that is based on the assumption that the particle size distribution has the Junge form throughout its evolution has several advantages. First, it mimics the distributions predicted by the sectional model. Second, particles are allowed to have different sizes, which permits estimation of flocculation times for encounter due to differential settling. Finally, the aggregation equations become simplified.

The evolution of the suspension is tracked based on the rate of loss of particles from the first section,

$$\frac{dn_1}{d\tau} = -n_1 \sum_{j=1}^{k} \hat{\beta}_{1,j} n_j \tag{15}$$

where k is the largest section containing particles. Initially, all of the mass resides in the first section. As the number of particles in that section begins to decrease, the equivalent mass is put into the second section, so that the total mass is conserved and $k = 2$. When the mass of particles in the second section reaches that in the first, the mass in the first and second sections are kept equal. The subsequent mass lost from sections 1 and 2 is put into the third section ($k = 3$) until such a time as the mass in the first three sections is equal. This continues until there is equal mass in $h - 1$ sections, at which time all of the mass lost from these sections is put into the last section.

By assuming a form of the size distribution, the number concentration of particles in any section is related to the number concentration of particles in the first. For those sections that contain equal total volume, the number concentration is given by

$$n_i = \frac{n_1 v_0}{2^{i-1} v_0} = 2^{1-i} n_1. \tag{16}$$

The total volume in the kth section is calculated based on the total volume of particles in the system, V_T, using the equation

$$V_T = (k-1) n_1 v_0 + n_k 2^{k-1} v_0. \tag{17}$$

Because the system of equations described in Eq. (15) consists of a single differential equation, a simple fourth-order Runge–Kutta solver from Press *et al.* (1992) is used to step the equation forward in time. At each time step, n_1 and k are evaluated, and the volume is distributed accordingly. This model is referred to as the 'reduced' model, and the dimensionless flocculation time it estimates is given the symbol τ_J.

4 Analysis

4.1. Model runs

Full-model dimensionless flocculation times (τ_B) are compared to reduced-model dimensionless flocculation times (τ_J) for aggregation with and without settling losses.

Table 1
Model inputs with $d_{max} = 10$ mm

Name	h	$D3$	d_0 (μm)	ρ_s (kg m^{-3})
A1	14	1.5	24.6	1185
B1	16	1.5	9.8	1636
C1		1.6	15.1	1199
D1	18	1.6	6.3	1586
E1		1.7	9.8	1185
F1	20	1.6	2.7	2890
G1		1.7	4.3	1469
H1		1.8	6.6	1154

Five model inputs affect flocculation time: d_0,G, $D3$, ρ_s, and the size of the largest allowable particle, which is determined by the number of sections used, h. Because large particles dominate aggregation, the maximum particle diameter and maximum settling velocity must be set to realistic values. From Eq. (13), the maximum particle diameter is a function of $D3$ and h, i.e.

$$d_{max} = d_0(2^{h-1})^{1/D3}. \tag{18}$$

The value of d_0 is calculated based on $d_{max} = \{10, 1, 0.1 \text{ mm}\}$, values that are based on the observed range of floc sizes (Dyer *et al.*, 1996). The expression

$$w_{s_{max}} = \frac{(\rho_s - \rho) g d_0^2}{18\mu} \left(\frac{d_{max}}{d_0}\right)^{D3-1}, \tag{19}$$

is used to calculate the value of ρ_s that gives a maximum, commonly observed settling velocity of 1 mm s^{-1} (ten Brinke, 1994; Syvitski *et al.*, 1995; Hill *et al.*, 1997). (Hill *et al.*, 1998) suggest that this settling velocity reflects the control of maximal floc size by stresses on sinking particles.) Only those inputs that give reasonable density values, ranging from $\rho_s = 1100$ kg m^{-3} for diatoms (Smayda, 1970) to a typical mineral value of $\rho_s = 3000$ kg m^{-3} (Hurlbut and Klein, 1977), are used. The lists of test cases are shown in Tables 1–3. For given $D3$ and h values, the relative importance of turbulent shear encounter is varied by changing the shear rate, $G = \{0.1, 0.5, 1.0, 5.0, 10.0 \text{ s}^{-1}\}$. These shear rates span deep-sea nepheloid-layer values of 0.084 s^{-1} (McCave, 1984) to continental shelf values of ~ 10 s^{-1} (Milligan, 1996).

4.2. Statistics

In order for the method of estimation developed here to be useful for predicting the flocculation time, the correction that directly relates τ_J to τ_B must be determined. This is achieved using multiple linear regression. If the relationship between the two dimensionless flocculation times is second order then

$$\mathbf{y} = B_0 + B_1\mathbf{x}_1 + B_2\mathbf{x}_2 + \cdots + B_m\mathbf{x}_m + B_{m+1}\mathbf{x}_1^2 + \cdots + B_{2m}\mathbf{x}_1\mathbf{x}_m + B_{2m+1}\mathbf{x}_2^2 + B_{2m+2}\mathbf{x}_2\mathbf{x}_3 + \cdots + B_{2m+(m-1)}\mathbf{x}_2\mathbf{x}_m + \cdots + B_k\mathbf{x}_m^2,$$

Table 2
Model inputs with $d_{max} = 1$ mm

Name	h	$D3$	d_0 (μm)	ρ_s (kg m^{-3})
A2	10	1.5	15.6	1974
B2		1.6	20.3	1465
C2		1.7	25.5	1251
D2		1.8	31.3	1152
E2		1.9	37.5	1103
F2	12	1.6	8.5	2484
G2		1.7	11.3	1660
H2		1.8	14.5	1331
I2		1.9	18.1	1187
J2		2.0	22.1	1118
K2	14	1.7	5.0	2839
L2		1.8	6.7	1781
M2		1.9	8.7	1373
N2		2.0	11.0	1201
O2		2.1	13.7	1122
P2	16	1.8	3.1	2914
Q2		1.9	4.2	1790
R2		2.0	5.5	1367
S2		2.1	7.1	1193
T2		2.2	8.9	1115
U2	18	1.9	2.0	2719
V2		2.0	2.8	1699
W2		2.1	3.7	1321
X2		2.2	4.7	1168
Y2		2.3	6.0	1101
Z2	20	2.0	1.4	2364
AA2		2.1	1.9	1554
BB2		2.2	2.5	1256
CC2		2.3	3.3	1136

Table 3
Model inputs with $d_{max} = 0.1$ mm

Name	h	$D3$	d_0 (μm)	ρ_s (kg m^{-3})
A3	10	2.2	5.9	2808
B3		2.3	6.6	2260
C3		2.4	7.4	1908
D3		2.5	8.2	1674
E3	12	2.3	3.6	2903
F3		2.4	4.2	2269
G3		2.5	4.7	1878
H3	14	2.4	2.3	2781
I3		2.5	2.7	2147
J3	16	2.5	1.6	2503
K3	18	2.5	0.9	2972

where $\mathbf{y}$ is the response variable, i.e. τ_B, $\mathbf{x}_1$ is τ_J, and the other predictors ($\mathbf{x}_2$ through $\mathbf{x}_k$) may be $D3$ or any of the other model inputs that affect the flocculation time. The coefficients $B_0, \ldots, B_k$ are the parameters of least-squares regression.

It must be stressed that the predictors for each correction are not chosen because of their physical significance. Flocculation times calculated by the various models are all estimates of the same quantity, but they are entirely independent of one another. The corrections are used purely for predictive purposes, so the form of the equations chosen is based only on how robustly they relate the estimate to the Batterham *et al.* model value. Also, the calculated parameters are not used to infer the relative significance of one term with respect to another.

Dimensionless flocculation time τ_J is a function of $D3$, G, and h, and these inputs are also variables in the regression equation. Therefore, any term containing τ_J will tend to be correlated with terms containing D^3, G, and h. Correlation among predictors is reduced by standardizing each array of predictor observations by its mean and standard deviation. That is, mean and standard deviation of $\mathbf{x}$, respectively. A regression equation based on standarised predictors can easily be converted back into non-standardized.

Statistical analysis is performed using MINITAB. This statistical package provides a systematic method for determining which predictors are required to properly describe the relationship between the two calculated flocculation times. The criteria used to select the best regression equations are C_p and s^2. The C_p statistic is a function of the number of parameters in a model and the error mean square, s^2. According to Walpole and Myers (1989), the C_p statistic "is developed from considerations of the proper compromise between excessive bias incurred when one underfits and excessive prediction variance produced when one overfits". If $C_p > p$, where p is the number of parameters $(k + 1)$, then the model is biased due to underfit; if $C_p \leqslant p$, then the model is a reasonable one. For comparable values of C_p, the model with the lower s^2 value is preferable.

5. Results and discussion

5.1. Aggregation without settling losses

Plots of τ_B vs. τ_J show that there is a highly linear relationship between the two with changing shear rate (Fig. 3). The cases shown all have the same value of maximum floc diameter, $d_{max} = 1$ mm, and within each plot, h is constant. Regression lines are drawn through points of varying G within the same case. The slope of the regression line increases regularly with increasing $D3$. For $D3 < 2.0$, τ_J generally underestimates τ_B, while for $D3 > 2.0$, τ_J overestimates τ_B. By visual inspection, the change in slope with h is less pronounced. This suggests that the relationship between the full and reduced models is more strongly determined by the fractal dimension and that increasing h merely increases τ_{floc} for both models.

The increase in slope with $D3$ can be explained by examining mass distributions for several cases. They show that the simplifying assumption of a perfectly

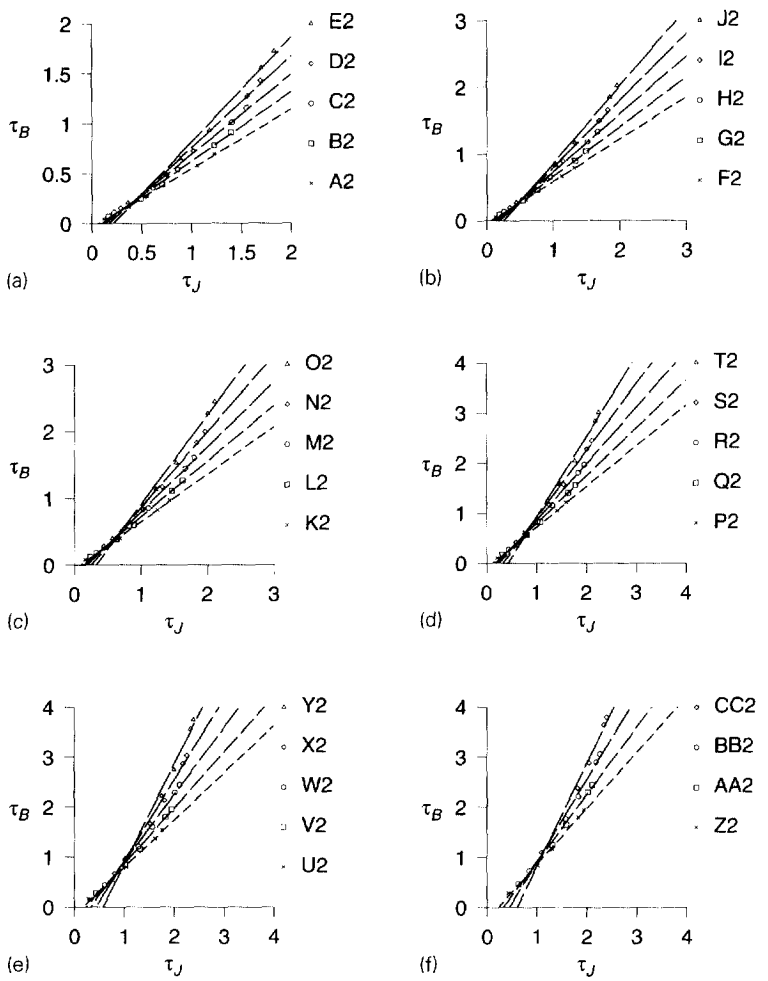

Fig. 3. Comparison of dimensionless flocculation times for turbulent shear and differential settling encounter calculated using the full model (τ_B) and the Junge-dispersion approach (τ_J) for all cases with maximum diameter of $d_{max} = 1$ mm. Each plot shows the cases with the same number of sections. Regression lines are drawn through points within the same case ($R^2 > 0.99$ for all regression lines).

Junge-distributed size distribution is not supported by the full model for all values of $D3$. Instead, the initial slope of the mass distribution varies with $D3$. For cases with low $D3$, the slope of the mass distribution is negative, i.e., there is more mass in the smallest sections than in intermediate sections, while for cases with high $D3$, the slope of the mass distribution is positive. For cases with $D3 \approx 2.0$, the slope is very close to zero for small i. Therefore, the general trend of an increase in the slope of the relationship between τ_B and τ_J corresponds to an increase in the initial slope of the mass distribution predicted by the full model. For $D3 = 2.0$, the slope of the mass distribution is zero, and there is a near 1 : 1 correspondence between τ_B and τ_J.

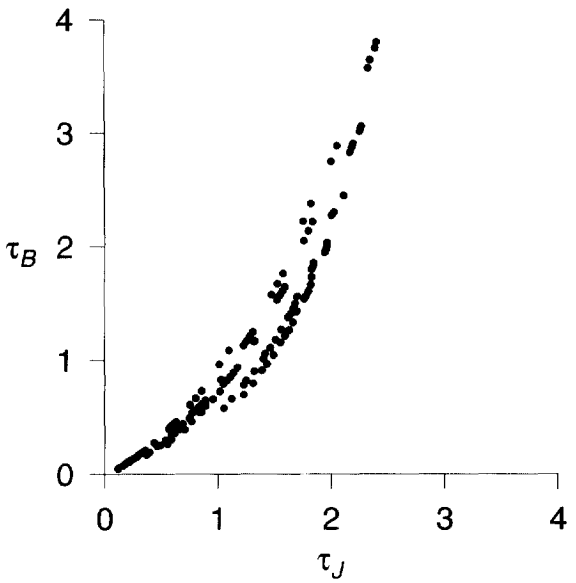

Fig. 4. Comparison of dimensionless flocculation times calculated using the full model (τ_B) and the Junge-dispersion approach (τ_J) for all cases with encounter due to turbulent shear for maximum diameter of $d_{max} = 1$ mm. Refer to Table 2 for a description of the cases shown.

All of the cases with $d_{max} = 1$ mm show an overall relationship between τ_B and τ_J that is not linear, but of a higher order (Fig. 4). While we would expect all dimensionless flocculation times to be of order 1, it is unclear why the range in τ_{floc} for both methods should be so narrow; all are between ~0 and 4. Possibly it is because of the way in which the maximum floc size is limited. If a second-order equation is fit to this curve, then a total of 14 terms is possible. These terms arise from the first and second powers of the predictor variables (τ_J, G, $D3$, and h) and second-order interaction terms. To obtain an acceptable value of C_p, 11 variables must be included, for a total of 12 parameters. The inclusion of more variables does not significantly reduce s^2. The regression equation is

$$\begin{aligned}\tau_B = & -2.438\,\tau_J - 0.152\,G + 1.433\,D3 - 0.202\,h \\ & + 0.236\,\tau_J^2 - 0.842\,D3^2 - 0.208\,\tau_J G + 1.452\,\tau_J D3 \\ & + 0.312\,G\,D3 - 0.002\,G\,h + 0.102\,D3\,h + 0.427, \end{aligned} \tag{20}$$

where h is calculated using

$$h = D3 \log_2\left(\frac{d_{max}}{d_0}\right) + 1. \tag{21}$$

Similarly for $d_{max} = 10\,mm$, the best fit is given by

$$\begin{aligned}\tau_B = & -0.941\,\tau_J - 0.030\,G - 0.279\,D3 - 0.018\,h \\ & + 0.076\,\tau_J^2 + 0.0006\,G^2 + 0.0006\,h^2 - 0.023\,\tau_J G \\ & + 0.964\,\tau_J D3 - 0.005\,\tau_J h + 0.035\,G D3 + 0.554. \end{aligned} \tag{22}$$

For $d_{max} = 0.1\,mm$, all 14 variables must be included, and the best model is

$$\begin{aligned}\tau_B = & -3.010\,\tau_J - 0.411\,G + 1.510\,D3 - 0.434\,h \\ & + 0.424\,\tau_J^2 + 0.004\,G^2 - 0.849\,D3^2 - 0.004\,h^2 \\ & - 0.288\,\tau_J G + 1.05\,\tau_J D3 + 0.047\,\tau_J h + 0.337\,G D3 \\ & + 0.016\,G h + 0.222\,D3\,h + 0.794. \end{aligned} \tag{23}$$

5.2. Aggregation with settling losses

A number of cases given in Tables 1–3 were re-run with the inclusion of settling loss, with the model equations modified to include an additional loss term according to Friedlander (1977). For large values of z (suspension thickness), settling loss is insignificant and the total volume of particles in suspension decreases only slightly throughout the evolution of the size distribution. As a result, d_{50} increases in the characteristic way. As z decreases and settling-loss rates grow, total volume decreases significantly, and the suspension no longer flocculates. Because settling removes the largest particles preferentially, median diameter remains small. However, the time at which the transition to the flocculated state begins is more or less the same regardless of the rate of settling loss.

The ratio of time scales for aggregation and sinking provides a tool for gauging whether or not sinking losses are important. This ratio has the form

$$\frac{t_{floc}}{t_{sink}} = \frac{t_{floc}\,w_{s_{max}}}{z}. \tag{24}$$

where t_{floc} is determined based on the dimensionless flocculation time predicted using the Junge-distribution method (τ_J) and re-dimensionalized using the expression given by Eq. (11). If this ratio is less than one, then the time scale for sinking is greater than the flocculation time, and sinking losses are insignificant. If, however, the ratio is close to or greater than one, then sinking losses become important, and the mass of particles in suspension cannot be assumed to be constant (Fig. 5).

6. Implementation

6.1. Comparison of reduced model with correction to full model

To compare the flocculation times predicted by the two models, inputs for new cases were created using a random number generator in the computer algebra system

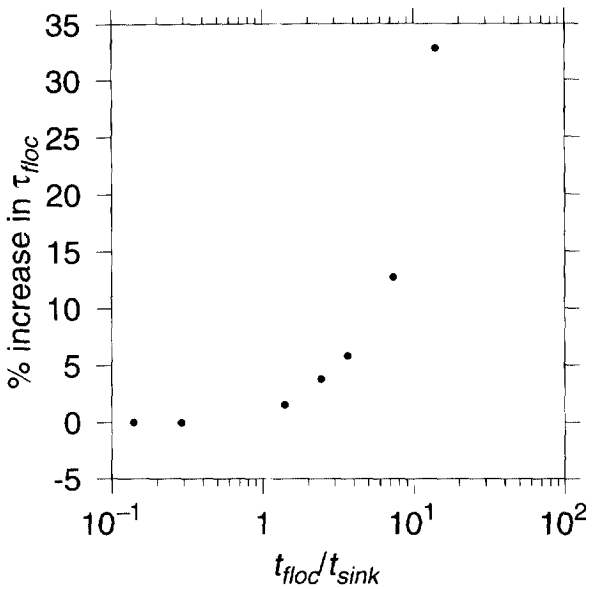

Fig. 5. Time-scale ratio for case C1 (see Table 1) plotted versus percentage increase in dimensionless flocculation time from its no-loss value.

Maple. A function within this package selects random numbers from within a user-specified range. Values of h, $D3$, d_{max}, and G were generated from within the range of values used in the previous cases, and d_0 and ρ_s were calculated from these. Again, only those cases with $1100\,\mathrm{kg\,m^{-3}} < \rho_s < 3000\,\mathrm{kg\,m^{-3}}$ were allowed (Table 4). The corrected reduced model gives dimensionless flocculation times generally within ~3% of the full model value. The relative difference does not exceed 6% for the cases tested (Table 5).

6.2. *Revisiting published flocculation times*

Previous studies use half-life to calculate representative flocculation times. McCave (1985) compares time scales for particle removal for three particle sizes ($d_0 = \{1, 5, 20\,\mu\mathrm{m}\}$) and conditions representative of bottom boundary layers. He calculates a half-life for aggregation due to turbulent shear only for $d_0 = 20\,\mu\mathrm{m}$, as Brownian motion dominates for particles smaller than 8 μm (McCave, 1984). With values of $C_0 = 100\,\mu\mathrm{g\,l^{-1}}$, $G = 0.084\,\mathrm{s^{-1}}$, $\rho_s = 1.282\,\mathrm{g\,cm^{-3}}$, and $\alpha = 0.1$, he calculates a half-life of 27 years. In contrast, the time scale for deposition for this case is only 12 days ($z = 50\,\mathrm{m}$, $w_s = 4.09 \times 10^{-3}\,\mathrm{cm\,s^{-1}}$); consequently, McCave concludes that deposition is the dominant removal mechanism for particles of this size.

A different result is obtained using the Junge-distribution model. With McCave's reported maximum floc size of 2–4 mm and an initial number concentration of $N_0 = 1.9 \times 10^{7}\,\mathrm{m^{-3}}$, the range of flocculation times presented in Table 6 is calculated.

Table 4
Model inputs for new cases not used in the development of the predictive regression equations.

#	h	d_{max}(mm)	$D3$	G (s^{-1})	d_0 (μm)	ρ_s (kg m^{-3})
1	11	0.10	2.41	6.68	5.635	2036
2	18	1.0	2.04	4.31	3.100	1504
3	16	1.0	1.81	1.42	3.201	2742
4	11	1.0	1.54	1.68	11.10	2345
5	17	1.0	2.07	7.82	4.712	1302
6	10	1.0	1.88	7.91	36.22	1110
7	19	10.0	1.80	5.81	9.766	1110
8	15	1.0	1.90	2.13	6.052	1540
9	12	1.0	2.00	8.95	22.10	1118
10	15	1.0	1.76	9.13	4.031	2744
11	11	1.0	1.76	3.28	19.48	1277
12	10	1.0	1.86	1.14	34.95	1118
13	13	1.0	2.07	3.95	17.98	1112
14	10	1.0	1.66	5.52	23.33	1317
15	11	0.10	2.39	5.01	5.501	2111
16	17	10.0	1.59	9.68	9.349	1377
17	19	1.0	2.10	5.50	2.629	1420
18	16	10.0	1.56	9.55	12.75	1305
19	18	10.0	1.70	4.06	9.766	1185
20	11	0.10	2.27	7.49	4.719	2739

Table 5
Dimensionless flocculation times calculated using the Batterham *et al.* (1981) model (τ_B) and the Junge-distribution method, corrected using the predictive equations ($\tau_{Jcorrected}$) for a number of new cases not used in the development of the predictive regression equations

#	τ_B	$\tau_{Jcorrected}$	$\Delta\tau/\tau_B$ (%)
1	2.202	2.192	0.4
2	1.945	1.997	− 2.7
3	0.689	0.649	5.8
4	0.367	0.378	− 3.0
5	2.245	2.309	2.9
6	1.617	1.639	− 1.4
7	1.366	1.346	1.4
8	1.143	1.140	0.2
9	2.006	2.095	− 4.4
10	1.097	1.150	− 4.8
11	0.995	0.980	1.5
12	0.902	0.870	3.5
13	2.049	2.106	− 2.8
14	0.940	0.887	5.6
15	1.887	1.893	− 0.3
16	0.856	0.844	1.4
17	2.322	2.371	− 2.1
18	0.802	0.789	1.6
19	1.060	1.055	0.5
20	1.813	1.817	− 0.2

Table 6
Flocculation times (t_{floc}) calculated using the Junge-distribution method and inputs from McCave (1985). For both values of maximum floc diameter (d_{max}), flocculation times are calculated with the maximum and minimum values of fractal dimension ($D3$) that produce values of component grain density in the specified range

d_{max}	$D3$	t_{floc}(yr)
1 mm	2.0	4.0
	1.5	4.1
10 mm	1.6	3.3
	1.5	2.1

Because fractal dimension is not reported, the maximum and minimum fractal dimensions that produce reasonable solids densities for each value of d_{max} are used. These flocculation times are considerably shorter than 27 years, but longer than the half-life for deposition, so McCave's conclusion remains unchallenged. However, if the mass concentration is increased to 10 mg, a concentration which is observed in bottom boundary layers in the deep sea (Hollister *et al.*, 1984), then the flocculation times presented above decrease by a factor of 100 and the depositional and flocculation time scales are of the same order.

Logan *et al.* (1995) compare half-lives from a mesocosm experiment and conclude that the characteristic sinking of diatom blooms is controlled by TEP. They measure concentrations and calculate half-lives for 6 days, after an initial incubation period of 6 days. For TEP on day 7, $\alpha = 0.21$, $N_0 = 1400\,\mathrm{ml}^{-1}$, and $d_0 = 20\,\mu\mathrm{m}$, while for phytoplankton, $\alpha = 0.015$, $N_0 \approx 220\,\mathrm{ml}^{-1}$, and $d_0 = 53\,\mu\mathrm{m}$. The shear rate in the tank is calculated to be $G = 1.3\,\mathrm{s}^{-1}$. On day 11, TEP concentration and diameter are $N_0 \approx 550\,\mathrm{ml}^{-1}$ and $d_0 = 112\,\mu\mathrm{m}$, and phytoplankton concentration is $N_0 \approx 2000\,\mathrm{ml}^{-1}$. The half-lives they calculate for TEP and phytoplankton on the seventh day are 2 days and 10 days, respectively, and for day 11, they calculate half-lives of 0.01 and 0.2 days.

The half-lives calculated by Logan *et al.* (1995) are better estimates of flocculation time than in the previous example (Table 7). Although flocculation times triple over the range of fractal dimensions, half-lives are consistently of the same order as flocculation times. This discrepancy likely results from the magnitude of the shear rate for each case. A deep-sea bottom boundary layer is a low-shear environment ($G = 0.084\,\mathrm{s}^{-1}$); thus differential settling encounter is the dominant mechanism in this situation. However, the half-life calculated is for turbulent shear encounter alone. On the other hand, a mesocosm is a relatively high-shear environment ($G = 1.3\,\mathrm{s}^{-1}$), where turbulent shear is a more important mechanism; consequently, half-life is a more appropriate estimate of flocculation time for this case.

6.3. *Limitations of method*

This new method for estimating flocculation time has several limitations, some of which are the same as those for the sectional model. For instance, neither the full nor

Table 7
Flocculation times calculated using the Junge-distribution method and inputs from Logan *et al.* (1995). Flocculation times are obtained using a maximum floc diameter of $d_{max} = 1$ mm and maximum and minimum values of fractal dimension ($D3$) that produce values of component grain density in the specified range. For day 11, component grain densities calculated using the Junge-distribution method for TEP were outside of the acceptable range for all values of $D3$

Day	Particle	$D3$	t_{floc} (d)
7	TEP	2.0	3.8
		1.5	1.0
	Phytoplankton	1.7	9.5
		1.5	6.1
11	Phytoplankton	1.7	1.0
		1.5	16.2 h

the reduced model includes particle disaggregation. Limiting the maximum particle size can be thought of as setting all sticking coefficients in sections larger than h to zero, so that any particle larger than $2^{h-1} v_0$ is broken instantly upon formation. However, particles smaller than $2^{h-1} v_0$ are also subject to breakup forces, and no attempt is made to include these forces into either model. Another limitation of both models is that only initially monodispersed suspensions can be modeled. Modeling truly polydispersed suspensions involves tracking individual component grains throughout the evolution of the size distribution. While it is possible to do this, such a model would be fundamentally different from population-balance type models and computationally expensive to run.

Other limitations are unique to the reduced model. One is that it does not allow both d_0 and ρ_s to be specified. This restriction is necessary to ensure that maximum floc size and settling velocity are limited to realistic values. However, there may be situations, e.g. diatom blooms, when mean size and density are known. Also, no dilution effects have been included into the reduced model. Dilution is distinct from settling loss in that there is no size discrimination. It is an important factor in the study of plumes.

7. Conclusions

The Bremer *et al.* (1995) formulation provides an easy method for calculating flocculation time, if one is willing to neglect differential settling encounter. It is a considerable improvement over half-life, which includes no effect of particle geometry. As these results have shown, fractal dimension is an important parameter in any calculation of flocculation time.

For a robust estimate of flocculation time, one in which both turbulent shear and differential settling are considered, the Junge-distribution model offers a fast method of calculation. On a SPARC station 10 Model 41, typical model run-time is reduced

from 1 to 2 h to between 15 and 30 s. Although the relationship between τ_J and τ_B varies, the regression equations provide corrected τ_J values to within $\sim 6\%$ of τ_B.

In addition to aggregation, processes such as sinking out of the water column, dilution, and particle breakup also contribute to changing number concentrations with time. For sinking loss, the ratio of flocculation time to sinking time determines whether the Junge-distribution method can be used. The effects of dilution and particle break up remain to be investigated.

References

Alldredge, A.L., McGillivary, P., 1991. The attachment probabilities of marine snow and their implications for particle coagulation in the ocean. Deep-Sea Research 38, 431–443.

Batterham, R.J, Hall, J.S., Barton, G., 1981. Pelletizing kinetics and simulation of full-scale balling circuits. In: Proceedings, 3rd International Symposium on Agglomeration, Nürnberg, Federal Republic of Germany, pp. A136–A150.

Birkner, F.B., Morgan, J.J., 1968. Polymer flocculation kinetics of dilute colloidal suspension. Journal of the American Water Works Association 60, 175–191.

Bremer, L.G.B., Walstra, P., van Vliet, T., 1995. Estimations of the aggregation time of various colloidal systems. Colloids and Surfaces A: Physicochemical and Engineering Aspects 99, 121–127.

Dealy, J.M., 1984. Official nomenclature for material functions describing the response of a viscoelastic fluid to various shearing and extensional deformation. Journal of Rheology 28, 181–195.

Dyer, K.R., Cornelisse, J., Dearnaley, M.P., Fennessy, M.J., Jones, S.E., Kappenberg, J., McCave, I.N., Pejrup, M., Puls, M., van Leussen, W., Wolfstein, K., 1996. A comparison of in situ techniques for estuarine floc settling velocity measurements. Journal of Sea Research 36, 15–29.

Friedlander, S.K., 1977. Smoke, Dust and Haze: Fundamentals of Aerosol Behavior. Wiley-Interscience, New York.

Han, M., Lawler, D.F., 1992. The (relative) insignificance of G in flocculation. Journal of the American Water Works Association 84, 79–91.

Hill, P.S., Nowell, A.R.M., 1995. Comparison of two models of aggregation in continental-shelf bottom boundary layers. Journal of Geophysical Research 100, 749–763.

Hill, P.S., Nowell, A.R.M., Jumars, P.A., 1992. Encounter rate by turbulent shear of particles similar in diameter to the Kolmogorov scale. Journal of Marine Research 50, 643–668.

Hill, P.S., Syvitski, J.P., Cowan, E.A., Powell, R.D., 1998. In situ observations of floc settling velocities in Glacier Bay, Alaska. Marine Geology 145, 85–94.

Hunt, J.R., Prediction of oceanic particle size distributions from coagulation and sedimentation mechanisms. In: Kavanaugh, M.C., Leckie, J.O., (Eds.), Particulates in Water. American Chemical Society, pp. 243–257.

Hurlbut, C.S., Klein, C., 1977. Manual of Mineralogy, 19th ed., Wiley, Toronto, 532 pp.

Jackson, G.A., 1990. A model of the formation of marine algal flocs by physical coagulation processes. Deep-Sea Research 37, 1197–1211.

Koh, P.T.L., Andrews, J.R.G., Uhlherr, P.H.T., 1987. Modelling shear-flocculation by population balances. Chemical Engineering Science 42, 353–362.

Kostoglou, M., Karabelas A.J., 1994. Evaluation of zero order methods for simulating particle coagulation. Journal of Colloid and Interface Science 163, 420–431.

Lerman, A., Carder, K.L., Betzer, P.R., 1977. Elimination of fine suspendoids in the oceanic water column, Earth and Planetary Science Letters 37, 61–70.

Li, X., Logan, B.E., 1997a. Collision frequencies of fractal aggregates with small particles by differential sedimentation. Environmental Science and Technology 31, 1229–1236.

Li, X., Logan, B.E., 1997b. Collision frequencies of fractal aggregates with small particles in a turbulently sheared fluid. Environmental Science and Technology 31, 1237–1243.

Lick, W., Lick, J., Ziegler, C.K., 1992. Flocculation and its effect on the vertical transport of fine-grained sediments. Hydrobiologia 235/236, 1–16.

Lick, W., Huang, H., 1993. Flocculation and the physical properties of flocs. In: Mehta, A.J., (Ed.), Nearshore and estuarine cohesive sediment transport, American Geophysical Union, Washington, DC, pp. 21–39.

Logan, B.E., Wilkinson, D.G., 1990. Fractal geometry of marine snow and other biological aggregates. Limnology and Oceanography 35, 130–136.

Logan, B.E., Passow, U., Alldredge, A.L., Grossart, H.-P., Simon, M., 1995. Rapid formation and sedimentation of large aggregates in predictable from coagulation rates (half-lives) of transparent exopolymer particles (TEP). Deep-Sea Research 42, 203–214.

McCave, I.N., 1984. Size spectra and aggregation of suspended particles in the deep ocean. Deep Sea Research 31, 329–352.

McCave, I.N., 1985. Mechanics of deposition of fine-grained sediments from nepheloid layers. Geo-Marine Letters 4, 243–245.

Meakin, P., 1991. Fractal aggregates in geophysics. Reviews of Geophysics 29, 317–354.

Milligan, T.G., 1996. A laboratory assessment of the relative importance of turbulence, particle composition and concentration in limiting maximal floc size and settling behaviour. Master's Thesis, Dalhousie University, 73 pp.

Oles, V., 1992. Shear-induced aggregation and breakup of polystyrene latex particles. Journal of Colloid and Interface Science 154, 351–358.

O'Melia, C.R., Tiller, C.L., 1993. Physicochemical Aggregation and Deposition in Aquatic Environments. In: Buffle, J., and van Leeuwan, H.P., (Eds.), Environmental particles, vol. 2, Lewis Publishers, pp. 353–386.

Press, W.H., Teukolsky, S.A., Vetterling, W.T., Flannery, B.P., 1992. Numerical Recipes in C: The Art of Scientific Computing. 2nd ed. Cambridge University Press, Melbourne, 994 pp.

Pruppacher, H.R., Klett, J.D., 1980. Microphysics of Clouds and Precipitation, D. Reidel, Dordrecht, 714 pp.

Saffman, P.G., Turner, J.S., 1956. On the collision of drops in turbulent clouds. Journal of Fluid Mechanics 1, 16–30.

Smayda, T.J., 1970. The suspension and sinking of phytoplankton in the sea. Oceanography and Marine Biology Annual Review 8, 353–414.

Smoluchowski, M., 1917. Versuch einer mathematischen Theorie der Koagulationskinetic kolloider Lösungen. Z. Phys. Chemie, 92.

Spicer, P.T., Pratsinis, S.E., 1996. Shear-induced flocculation: the evolution of floc structure and the shape of the size distribution at steady state. Water Research 30, 1049–1056.

Syvitski, J.P.M., Asprey, K.W., G LeBlanc, K.W., 1995. In situ characteristics of particles settling within a deep-water estuary. Deep-Sea Research II, 42, 223–256.

ten Brinke, W.B.M., 1994. Settling velocities of mud aggregation in the Oosterschelde Tidal Basin (The Netherlands), determined by a submersible video system, Estuarine Coastal and Shelf Science 39, 549–564.

Walpole, R.E., Myers, R.H., 1989. Probability and Statistics for Engineers and Scientists, 4th ed., MacMillan Publishing Company, New York.

Weilenmann, U., O'Melia, C.R., Stumm, W., 1989. Particle transport in lakes: models and measurements. Limnology and Oceanography 34, 1–18.

Appendix: Symbols

A	empirical constant in Junge density distribution function
b	empirical constant in Junge density distribution function
B	coefficient of least squares regression
C_0	initial particle mass concentration
C_p	Mallow's statistic
d	particle diameter
d_0	component particle diameter
d_{50}	median mass diameter
d_c	critical diameter
d_{max}	maximum particle diameter
$D3$	3-dimensional fractal dimension
E	contact efficiency
f	number-density distribution function
g	constant of gravitational acceleration
G	shear rate
h	number of sections
i	section number
j	section number
k	largest section containing particles
K	particle encounter rate
m	nondimensional particle mass concentration
n	nondimensional particle number concentration
N	particle number concentration
N_0	initial particle number concentration
p	number of parameters in least squares regression
s^2	error mean square
t	time
t_{floc}	flocculation time
t_{sink}	sinking time scale
v_s	solid volume within a floc
V	particle volume concentration
V_T	total particle volume concentration
w_s	settling velocity
$\mathbf{x}$	predictor variable in least squares regression
$\bar{x}$	mean
$\mathbf{y}$	response variable in least squares regression
z	depth of water column
α	sticking efficiency
β	encounter rate coefficient

$\hat{\beta}$	dimensionless encounter rate coefficient
ε	turbulent kinetic energy dissipation rate
μ	dynamic viscosity
ν	kinematic viscosity
ρ	density of suspending medium
ρ_p	floc density
ρ_s	component grain density
σ	standard deviation
τ	dimensionless time
τ_B	dimensionless flocculation time predicted using Batterham *et al.*'s model
τ_{floc}	dimensionless flocculation time
τ_J	dimensionless flocculation time predicted using Junge-dispersion assumption
ϕ_0	initial volume fraction